

OPEN ACCESS

Dose rate effects in the radiation damage of the plastic scintillators of the CMS hadron endcap calorimeter

To cite this article: V. Khachatryan *et al* 2016 *JINST* 11 T10004

View the [article online](#) for updates and enhancements.

Related content

- [Radiation hardness of plastic scintillators for the Tile Calorimeter of the ATLAS detector](#)
H Jivan, B Mellado, E Sideras-Haddad *et al.*
- [Radiation hardness of plastic scintillators for the Tile Calorimeter of the ATLAS detector](#)
H Jivan, E Sideras-Haddad, R Erasmus *et al.*
- [A comparative study of the radiation hardness of plastic scintillators for the upgrade of the Tile Calorimeter of the ATLAS detector](#)
S Liao, R Erasmus, H Jivan *et al.*

Recent citations

- [Geant4 simulation of a conceptual calorimeter based on secondary electron emission](#)
F. Ozok *et al*
- [The upgrade of the CMS hadron calorimeter with silicon photomultipliers](#)
N. Strobbe

TECHNICAL REPORT

Dose rate effects in the radiation damage of the plastic scintillators of the CMS hadron endcap calorimeter

V. Khachatryan,^a A.M. Sirunyan,^a A. Tumasyan,^a A. Litomin,^b V. Mossolov,^b N. Shumeiko,^{b,1} M. Van De Klundert,^c H. Van Haeveermaet,^c P. Van Mechelen,^c A. Van Spilbeeck,^c G.A. Alves,^d W.L. Aldá Júnior,^d C. Hensel,^d W. Carvalho,^e J. Chinellato,^e C. De Oliveira Martins,^e D. Matos Figueiredo,^e C. Mora Herrera,^e H. Nogima,^e W.L. Prado Da Silva,^e E.J. Tonelli Manganote,^e A. Vilela Pereira,^e M. Finger,^f M. Finger Jr.,^f S. Jain,^f R. Khurana,^f G. Adamov,^g Z. Tsamalaidze,^{g,2} U. Behrens,^h K. Borras,^h A. Campbell,^h F. Costanza,^h P. Gunnellini,^h A. Lobanov,^h I.-A. Melzer-Pellmann,^h C. Muhl,^h B. Roland,^h M. Sahin,^h P. Saxena,^h V. Hegde,ⁱ K. Kotheke,ⁱ S. Pandey,ⁱ S. Sharma,ⁱ S.B. Beri,^j B. Bhawandeep,^j R. Chawla,^j A. Kalsi,^j A. Kaur,^j M. Kaur,^j G. Walia,^j S. Bhattacharya,^k S. Ghosh,^k S. Nandan,^k A. Purohit,^k M. Sharan,^k S. Banerjee,^l S. Bhattacharya,^l S. Bhowmik,^l S. Chatterjee,^l P. Das,^l R.K. Dewanjee,^l S. Jain,^l S. Kumar,^l M. Maity,^l G. Majumder,^l P. Mandakini,^l M. Patil,^l T. Sarkar,^l A. Saikh,^l S. Sezen,^m A. Juodagalvis,ⁿ S. Afanasiev,^o P. Bunin,^o Y. Ershov,^o I. Golutvin,^o A. Malakhov,^o P. Moisenz,^{o,1} V. Smirnov,^o A. Zarubin,^o M. Chadeeva,^p R. Chistov,^p M. Danilov,^p E. Popova,^p V. Rusinov,^p Yu. Andreev,^q A. Dermenev,^q A. Karneyeu,^q N. Krasnikov,^q D. Tlisov,^q A. Toropin,^q V. Epshteyn,^r V. Gavrilov,^r N. Lychkovskaya,^r V. Popov,^r I. Pozdnyakov,^r G. Safronov,^r M. Toms,^r A. Zhokin,^r H. Flacher,^s A. Baskakov,^t A. Belyaev,^t E. Boos,^t M. Dubinin,^{t,3} L. Dudko,^t A. Ershov,^t A. Gribushin,^t A. Kaminskiy,^t V. Klyukhin,^t O. Kodolova,^t I. Lokhtin,^t I. Miagkov,^t S. Obraztsov,^t S. Petrushanko,^t V. Savrin,^t A. Snigirev,^t V. Andreev,^u M. Azarkin,^u I. Dremin,^u M. Kirakosyan,^u A. Leonidov,^u A. Terkulov,^u S. Bitiukov,^v D. Elumakhov,^v A. Kalinin,^v V. Krychkin,^v P. Mandrik,^v V. Petrov,^v R. Ryutin,^v A. Sobol,^v S. Troshin,^v A. Volkov,^v A. Adiguzel,^w N. Bakirci,^{w,4} S. Cerci,^{w,5} S. Damarseckin,^w Z.S. Demiroglu,^w C. Dozen,^w I. Dumanoglu,^w E. Eskut,^w S. Girgis,^w G. Gokbulut,^w Y. Guler,^w I. Hos,^w E.E. Kangal,^w O. Kara,^w A. Kayis Topaksu,^w U. Kiminsu,^w M. Oglakci,^w G. Onengut,^w K. Ozdemir,^{w,6} S. Ozturk,^{w,7} A. Polatoz,^w D. Sunar Cerci,^{w,5} B. Tali,^{w,5} H. Topakli,^{w,4} S. Turkcapar,^w I.S. Zorbakir,^w C. Zorbilmez,^w B. Bilin,^x B. Isildak,^x G. Karapinar,^x A. Murat Guler,^x K. Ocalan,^{x,8} M. Yalvac,^x M. Zeyrek,^x

¹Deceased.²Also Joint Institute for Nuclear Research, Dubna, Russia.³Also California Institute of Technology, Pasadena, U.S.A.⁴Also Tokat University, Tokat, Turkey.⁵Also Adiyaman University, Adiyaman, Turkey.⁶Also Piri Reis University, Turkey.⁷Also Gaziosmanpasa University, Tokat, Turkey.⁸Also Necmettin Erbakan University, Konya, Turkey.

E. Gülmez,^y M. Kaya,^{y,9} O. Kaya,^{y,10} E.A. Yetkin,^{y,11} T. Yetkin,^{y,12} K. Cankocak,^z S. Sen,^z A. Boyarintsev,^{aa} B. Grynyov,^{aa} L. Levchuk,^{ab} V. Popov,^{ab} P. Sorokin,^{ab} A. Borzou,^{ac} K. Call,^{ac} J. Dittmann,^{ac} K. Hatakeyama,^{ac} H. Liu,^{ac} N. Pastika,^{ac} O. Charaf,^{ad} S.I. Cooper,^{ad} C. Henderson,^{ad} P. Rumerio,^{ad,13} C. West,^{ad} D. Arcaro,^{ae} D. Gastler,^{ae} E. Hazen,^{ae} J. Rohlf,^{ae} L. Sulak,^{ae} S. Wu,^{ae} D. Zou,^{ae} J. Hakala,^{af} U. Heintz,^{af} K.H.M. Kwok,^{af} E. Laird,^{af} G. Landsberg,^{af} Z. Mao,^{af} J.W. Gary,^{ag} S.M. Ghiasi Shirazi,^{ag} F. Lacroix,^{ag} O.R. Long,^{ag} H. Wei,^{ag} R. Bhandari,^{ah} R. Heller,^{ah} D. Stuart,^{ah} J.H. Yoo,^{ah} A. Apresyan,^{ai} Y. Chen,^{ai} J. Duarte,^{ai} M. Spiropulu,^{ai} D. Winn,^{aj} S. Abdullin,^{ak} S. Banerjee,^{ak} F. Chlebana,^{ak} J. Freeman,^{ak} D. Green,^{ak} D. Hare,^{ak} J. Hirschauer,^{ak} U. Joshi,^{ak} D. Lincoln,^{ak} S. Los,^{ak} K. Pedro,^{ak} W.J. Spalding,^{ak} N. Strobbe,^{ak} S. Tkaczyk,^{ak} A. Whitbeck,^{ak} S. Linn,^{al} P. Markowitz,^{al} G. Martinez,^{al} M. Bertoldi,^{am} S. Hagopian,^{am} V. Hagopian,^{am} T. Kolberg,^{am} M.M. Baarmand,^{an} D. Noonan,^{an} T. Roy,^{an} F. Yumiceva,^{an} B. Bilki,^{ao,14} W. Clarida,^{ao} P. Debbins,^{ao} K. Dilsiz,^{ao} S. Durgut,^{ao} R.P. Gandrajula,^{ao} M. Haytmyradov,^{ao} V. Khristenko,^{ao} J.-P. Merlo,^{ao} H. Mermerkaya,^{ao,15} A. Mestvirishvili,^{ao} M. Miller,^{ao} A. Moeller,^{ao} J. Nachtman,^{ao} H. Ogul,^{ao} Y. Onel,^{ao} F. Ozok,^{ao,16} A. Penzo,^{ao} I. Schmidt,^{ao} C. Snyder,^{ao} D. Southwick,^{ao} E. Tiras,^{ao} K. Yi,^{ao} A. Al-bataineh,^{ap} J. Bowen,^{ap} J. Castle,^{ap} W. McBrayer,^{ap} M. Murray,^{ap} Q. Wang,^{ap} K. Kaadze,^{aq} Y. Maravin,^{aq} A. Mohammadi,^{aq} L.K. Saini,^{aq} A. Baden,^{ar} A. Belloni,^{ar} S.C. Eno,^{ar,17} C. Ferraioli,^{ar} T. Grassi,^{ar} N.J. Hadley,^{ar} G.-Y. Jeng,^{ar} R.G. Kellogg,^{ar} J. Kunkle,^{ar} A. Mignerey,^{ar} F. Ricci-Tam,^{ar} Y.H. Shin,^{ar} A. Skuja,^{ar} M.B. Tonjes,^{ar} Z.S. Yang,^{ar} A. Apyan,^{as} K. Bierwagen,^{as} S. Brandt,^{as} M. Klute,^{aq} X. Niu,^{as} R.M. Chatterjee,^{at} A. Evans,^{at} E. Frahm,^{at} Y. Kubota,^{at} Z. Lesko,^{at} J. Mans,^{at} N. Ruckstuhl,^{at} A. Heering,^{au} D.J. Karmgard,^{au} Y. Musienko,^{au,2} R. Ruchti,^{au} M. Wayne,^{au} A.D. Benaglia,^{av} T. Medvedeva,^{av} K. Mei,^{av} C. Tully,^{av} A. Bodek,^{aw} P. de Barbaro,^{aw} M. Galanti,^{aw} A. Garcia-Bellido,^{aw} A. Khukhunaishvili,^{aw} K.H. Lo,^{aw} D. Vishnevskiy,^{aw} M. Zielinski,^{aw} A. Agapitos,^{ax} J.P. Chou,^{ax} E. Hughes,^{ax} H. Saka,^{ax} D. Sheffield,^{ax} N. Akchurin,^{ay} J. Damgov,^{ay} F. De Guio,^{ay} P.R. Duderu,^{ay} J. Faulkner,^{ay} E. Gurpinar,^{ay} S. Kunori,^{ay} K. Lamichhane,^{ay} S.W. Lee,^{ay} T. Libeiro,^{ay} S. Undleeb,^{ay} I. Volobouev,^{ay} Z. Wang,^{ay} S. Goadhouse,^{az} R. Hirosky^{az} and Y. Wang^{az} on behalf of CMS-HCAL collaboration

^a*Yerevan Physics Institute,
Yerevan, Armenia*

^b*National Centre for Particle and High Energy Physics,
Minsk, Belarus*

^c*Universiteit Antwerpen,
Antwerpen, Belgium*

⁹Also Marmara University, Turkey.

¹⁰Also Kafkas University, Kars, Turkey.

¹¹Also Istanbul Bilgi University, Turkey.

¹²Also Yildiz Technical University, Turkey.

¹³Also CERN, European Organization for Nuclear Research, Geneva, Switzerland.

¹⁴Also Argonne National Laboratory, Argonne, U.S.A.

¹⁵Also Erzincan University, Erzincan, Turkey.

¹⁶Also Mimar Sinan University, Istanbul, Turkey.

¹⁷Corresponding author.

- ^d*Centro Brasileiro de Pesquisas Fisicas,
Rio de Janeiro, Brazil*
- ^e*Universidade do Estado do Rio de Janeiro,
Rio de Janeiro, Brazil*
- ^f*Charles University,
Prague, Czech Republic*
- ^g*Institute of High Energy Physics and Informatization, Tbilisi State University,
Tbilisi, Georgia*
- ^h*Deutsches Elektronen-Synchrotron,
Hamburg, Germany*
- ⁱ*Indian Institute of Science Education and Research,
Pune, India*
- ^j*Panjab University,
Chandigarh, India*
- ^k*Saha Institute of Nuclear Physics,
Kolkata, India*
- ^l*Tata Institute of Fundamental Research-B,
Mumbai, India*
- ^m*Kyungpook National University,
Daegu, South Korea*
- ⁿ*Vilnius University,
Vilnius, Lithuania*
- ^o*Joint Institute for Nuclear Research,
Dubna, Russia*
- ^p*National Research Nuclear University Moscow Engineering Physics Institute,
Moscow, Russia*
- ^q*Institute for Nuclear Research,
Moscow, Russia*
- ^r*Institute for Theoretical and Experimental Physics,
Moscow, Russia*
- ^s*University of Bristol,
Bristol, United Kingdom*
- ^t*Moscow State University,
Moscow, Russia*
- ^u*P.N. Lebedev Physical Institute,
Moscow, Russia*
- ^v*State Research Center of Russian Federation, Institute for High Energy Physics,
Protvino, Russia*
- ^w*Cukurova University,
Adana, Turkey*
- ^x*Middle East Technical University, Physics Department,
Ankara, Turkey*
- ^y*Bogazici University,
Istanbul, Turkey*
- ^z*Istanbul Technical University,
Istanbul, Turkey*

- ^{aa}*Institute for Scintillation Materials of National Academy of Science of Ukraine,
Kharkov, Ukraine*
- ^{ab}*National Scientific Center, Kharkov Institute of Physics and Technology,
Kharkov, Ukraine*
- ^{ac}*Baylor University,
Waco, U.S.A.*
- ^{ad}*The University of Alabama,
Tuscaloosa, U.S.A.*
- ^{ae}*Boston University,
Boston, U.S.A.*
- ^{af}*Brown University,
Providence, U.S.A.*
- ^{ag}*University of California,
Riverside, Riverside, U.S.A.*
- ^{ah}*University of California,
Santa Barbara, Santa Barbara, U.S.A.*
- ^{ai}*California Institute of Technology,
Pasadena, U.S.A.*
- ^{aj}*Fairfield University,
Fairfield, U.S.A.*
- ^{ak}*Fermi National Accelerator Laboratory,
Batavia, U.S.A.*
- ^{al}*Florida International University,
Miami, U.S.A.*
- ^{am}*Florida State University,
Tallahassee, U.S.A.*
- ^{an}*Florida Institute of Technology,
Melbourne, U.S.A.*
- ^{ao}*The University of Iowa,
Iowa City, U.S.A.*
- ^{ap}*The University of Kansas,
Lawrence, U.S.A.*
- ^{aq}*Kansas State University,
Manhattan, U.S.A.*
- ^{ar}*University of Maryland,
College Park, U.S.A.*
- ^{as}*Massachusetts Institute of Technology,
Cambridge, U.S.A.*
- ^{at}*University of Minnesota,
Minneapolis, U.S.A.*
- ^{au}*University of Notre Dame,
Notre Dame, U.S.A.*
- ^{av}*Princeton University,
Princeton, U.S.A.*
- ^{aw}*University of Rochester,
Rochester, U.S.A.*

^{ax}*Rutgers, the State University of New Jersey,
Piscataway, U.S.A.*

^{ay}*Texas Tech University,
Lubbock, U.S.A.*

^{az}*University of Virginia,
Charlottesville, U.S.A.*

E-mail: eno@umd.edu

ABSTRACT: We present measurements of the reduction of light output by plastic scintillators irradiated in the CMS detector during the 8 TeV run of the Large Hadron Collider and show that they indicate a strong dose rate effect. The damage for a given dose is larger for lower dose rate exposures. The results agree with previous measurements of dose rate effects, but are stronger due to the very low dose rates probed. We show that the scaling with dose rate is consistent with that expected from diffusion effects.

KEYWORDS: Radiation damage to detector materials (solid state); Radiation-hard detectors; Scintillators and scintillating fibres and light guides; Calorimeters

ARXIV EPRINT: [1608.07267](https://arxiv.org/abs/1608.07267)

Contents

1	Introduction	1
2	Results from the CMS HE laser calibration	3
3	Results from a low dose rate irradiation at a ^{60}Co source	6
4	Comparison to previous results	7
5	Conclusions	8

1 Introduction

Plastic scintillators are widely used in detectors for experiments in high energy physics experiments due to their high light output, low cost, and versatility. However, they are also known to suffer from radiation damage (for a detailed review, see [1]). Typically, the light output of the scintillator decreases exponentially with the dose received, as in eq. (1.1):

$$L(d) = L_0 \exp(-d/D) \quad (1.1)$$

where $L(d)$ is the light output after receiving a dose d , L_0 is the light output before irradiation, and D is the exponential constant. The exponential constant D depends on the materials used in the construction of the scintillator and on its environmental history. Several results have also shown a dependence on dose rate [1–8]. The lowest dose rates probed by these measurements were a few krad/hr.

In this paper, we present results from scintillators used in the CMS hadron endcap calorimeter (HE) [9] irradiated at dose rates between ≈ 0.1 to a few times 10^{-4} krad/hr that indicate that the radiation damage can have a very strong dose rate dependence. We also present a measurement from an irradiation at a ^{60}Co source at a dose rate of 0.28 krad/hr.

Plastic scintillators consist of a plastic substrate, often polystyrene (PS) or polyvinyltoluene (PVT), into which wavelength shifting (WLS) fluors have been dissolved, usually a primary and a secondary fluor. When a charged particle traverses the scintillator, the molecules of the substrate are excited. This excitation can be transferred to the primary fluor radiatively in the deep UV at low concentrations or via the Förster mechanism [10] at higher concentrations. The primary fluor transfers the excitation radiatively to the secondary fluor. De-excitation of the secondary fluor generally produces light in the visible range, to match well with currently available photodetectors. The light must traverse the scintillator to reach the photodetector, and can be absorbed by “color centers” along its path.

Dose rates effects have been associated with oxygen diffusion [4, 11, 12]. The rate of diffusion depends on the substrate material and has a weak dependence on dose and on environmental

factors [11]. For unirradiated plastic, the diffusion rate for oxygen is 13 times slower for PVT than for PS [13]. Oxygen can increase the mobility of radicals created during irradiation when chemical bonds in the polymer of the substrate are broken, and can interact with radicals to affect the formation of color centers, which absorb light [12]. When oxygen is not present, cross linking is enhanced, and gel formation is increased [11]. These processes can affect the energy levels of the substrate, thus affecting the transfer mechanisms of the initial excitation produced by the charged particles being measured. When radicals are more mobile, they are more likely to reform good bonds, reducing their ill effects. (For a detailed review of radicals in polymers, see [14]). Those color centers that go away after a recovery period, whose length depends on temperature and the concentration of oxygen, are referred to as temporary damage. Color centers that remain after recovery are referred to as permanent damage. Oxygen tends to decrease temporary damage but increase permanent damage [1].

When the concentration of radicals is low, the penetration depth of oxygen into the substrate goes as [11]

$$z_0^2 = \frac{G}{R} \quad (1.2)$$

where

$$G = \frac{2VSP}{\Phi}, \quad (1.3)$$

R is the dose rate, V is the diffusion constant of the gas, S is the solubility constant of oxygen, P is the oxygen pressure, and Φ is the specific rate constant of active site formation. G is roughly independent of dose [4, 11].

For a simple configuration consisting of a piece of plastic scintillator with an alpha source on one side and a photodetector on the other, assuming the fraction of the thickness of the scintillator penetrated by the alpha is small, the light produced will traverse first a region penetrated by oxygen of depth z_0 , then a region the oxygen does not reach, of thickness $t - 2z_0$ where t is the thickness of the piece of scintillator, and finally another region with oxygen, before reaching the photodetector. If the inverse of the light absorption length when color centers are formed in the presence of oxygen is μ_1 and that formed independent of the presence of oxygen is μ_2 , the light output will be

$$L = L_0 \exp(-\mu_1(2z_0) - \mu_2 t). \quad (1.4)$$

The inverse absorption length μ is related to the density of color centers Y and the cross section for absorption of the light by the color center σ by

$$\mu = Y\sigma. \quad (1.5)$$

When the color center density Y is low, it depends on the chemical yield g , the density of the scintillator Q , and the dose d as

$$Y = gQd. \quad (1.6)$$

The light output is then

$$L(d) = L_0 \exp\left(-\left(g_1 Q_1 \sigma_1 2 \frac{\sqrt{G}}{\sqrt{R}}\right) d - (g_2 Q_2 \sigma_2 t) d\right) \quad (1.7)$$

and so the functional form of the dependence of the exponential constant on the dose rate is

$$D = \frac{\sqrt{R}}{A + B\sqrt{R}} \quad (1.8)$$

where $A = 2g_1Q_1\sigma_1\sqrt{G}$ and $B = g_2Q_2\sigma_2t$.

For a more complex arrangement, the dependence will not be as simple, but still might be expected to show a \sqrt{R} dependence at low dose rate and to approach a constant value at high dose rate.

2 Results from the CMS HE laser calibration

The HE is part of the CMS detector [15] at CERN’s Large Hadron Collider (LHC). It is a sampling calorimeter that uses brass as its passive material and scintillating tiles as its active material. It has 18 layers of active material, denoted layers 0 through 17, over most of its rapidity coverage. The zeroth layer of scintillator uses BC-408, a PVT-based scintillator from the Bicon division of the Saint Gobain corporation,¹ while the other layers use SCSN-81, a PS-based scintillator from Kuraray.² Figure 1 shows a schematic of the HE calorimeter.

The tiles are trapezoidal in shape. They contain a sigma groove that holds a 0.94 mm Y-11 (Kuraray) WLS fiber, mirrored on one end. Figure 2 shows a schematic of the tiles, arranged in a “mega tile” that holds individual tiles. The calorimeter spans the pseudorapidity region from 1.305 to 3. The tiles are labeled by their pseudorapidity by “tower number”, starting with 16 for the ones at lowest pseudorapidity and going to 29. Due to the geometry of the detector, layers 0 through 4 contain tiles corresponding to towers 17 through 29. Layers 5 through 17 do not have tower 29. Only Layers 5 through 10 contain tower 16, and layers 14 through 17 do not have tile 17 as well. The megatiles are inserted into the brass absorber of the HE. The tile thickness is 0.9 cm in layer 0 and 0.37 cm in the rest of the layers. The sizes range from roughly 10 cm × 10 cm to about 20 cm × 20 cm. Clear fibers carry the light to hybrid photodiodes (HPD) [16], and each HPD signal is digitized by a Charge Integrator and Encoder (QIE) [17].

The light output of the tiles was measured during the 2012 8 TeV run of the LHC. The total delivered integrated luminosity was 23.3 fb⁻¹, and was estimated as described in [18]. The time was estimated three different ways: using LHC 2012 run performance summaries that included information on total delivered luminosity and hours in stable beam, using detailed CMS Web Based Monitoring records for each fill parameter including delivered luminosity and time in fill, and using the peak luminosity, luminosity lifetime, and fill length values to correlate average lumi rate with peak lumi. All three methods delivered very similar results. The instantaneous luminosity was fairly constant during the run.

The light was measured using a laser calibration system, consisting of a triggerable nitrogen laser, a system of neutral density filters, and a light distribution system that delivers the UV light to the scintillator tiles in layers 1 and 7 via quartz fibers. Light was also injected directly into the HPDs. The laser light was injected during the run at times without collisions, between fills of the accelerator with protons.

¹Saint-Gobain Crystals, Courbevoie, France.

²Kuraray Corporation, Otemachi, Chiyoda-ku, Tokyo, 100-8115 Japan.

Eta Position of tiles

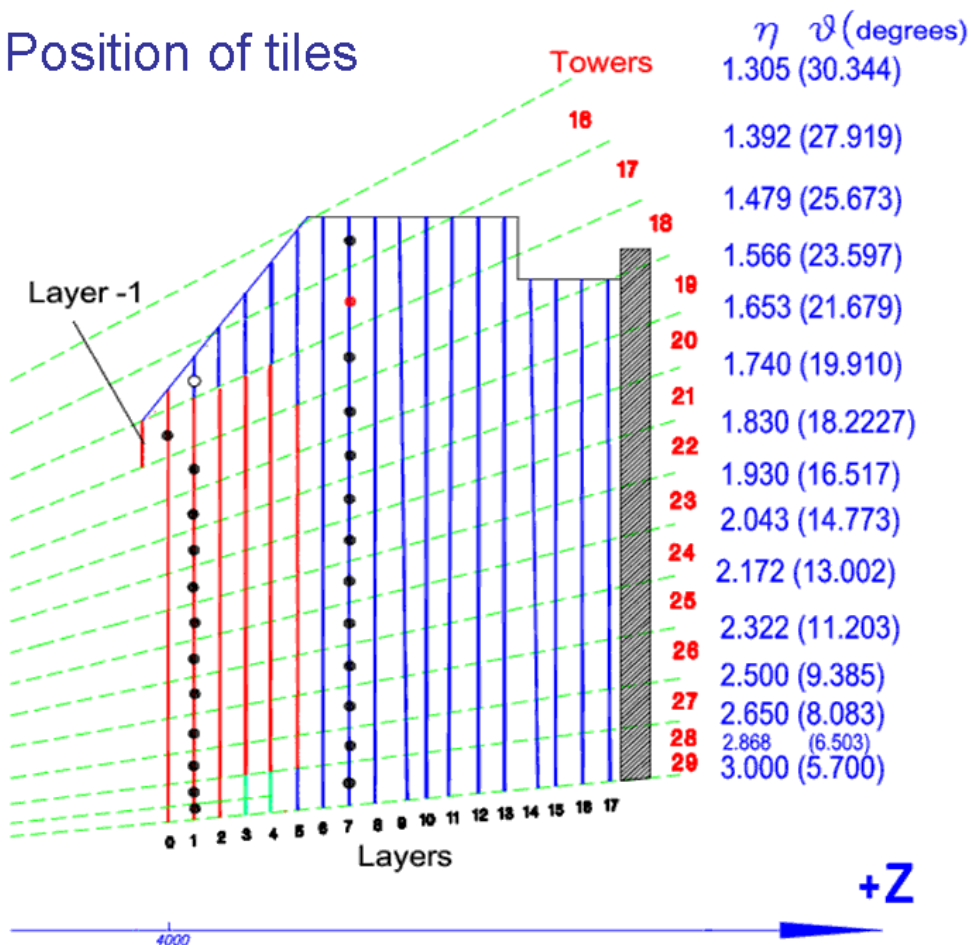


Figure 1. Schematic of the CMS hadron endcap calorimeter.

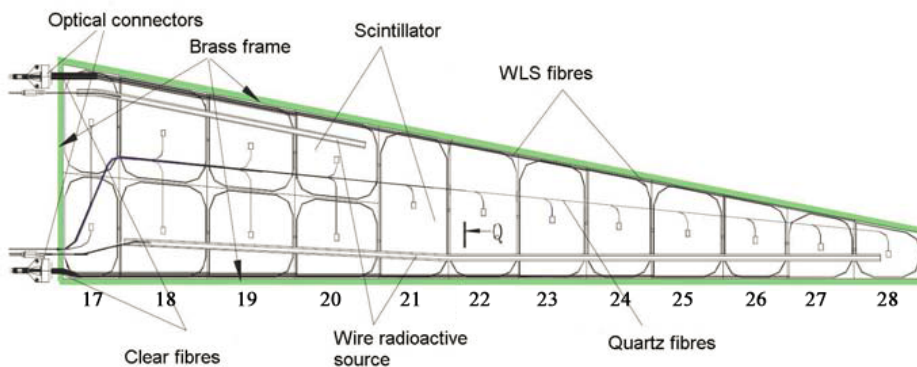


Figure 2. Schematic of the CMS hadron endcap calorimeter scintillator megatile tiles for tiles in layer 11 through 13. The numbers below the tiles represent the tower number. The megatiles in layers 0 through 4 have an additional tower at large η (tower 29). The megatiles in layers 5 through 10 contain tile 16 at low η . Layers 14 through 17 do not have tile 17.

Plots of the light output relative to the initial light output as a function of the accumulated integrated luminosity during the run are shown in figure 3. They show an exponential decrease in light output with integrated luminosity. After the end of the run, a few percent recovery was observed for the tiles with the largest damage. The data are not corrected for this effect.

Cross checks of the results from the laser calibration from calculations of the jet energy scale, a calibration using a ^{60}Co source after the end of the run, and a measurement looking at the energy distribution in the towers using data taken with a single electron trigger as a function of integrated luminosity give similar albeit less precise results.

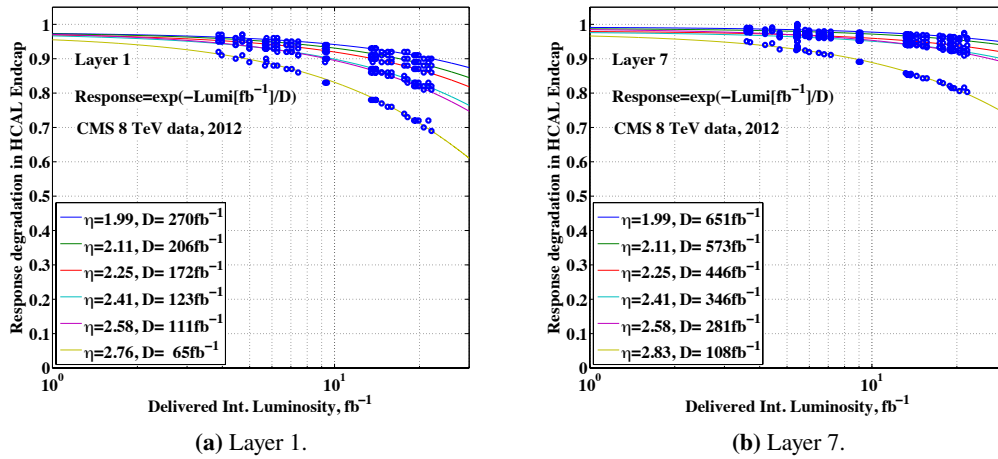


Figure 3. Ratio of light output to initial light output for tiles as a function of integrated luminosity, with extracted dose constant, for CMS hadron endcap calorimeter scintillators in Layer 1 (a) and in Layer 7 (b).

To convert the exponential constant in terms of integrated luminosity to an exponential constant in terms of dose, the dose received by the tile per unit integrated luminosity is needed. Predictions of the absorbed dose in HE scintillator layers were obtained using the Monte Carlo code FLUKA 2011.2c [19, 20]. The FLUKA predictions for collisions use a model that represents the HE in detail, with brass, Dural (Aluminium, Cu, Mg, and Mn), Tyvek, air, and scintillator layers. The absorber regions are represented as 80 mm thick brass ‘LK75’ layers (with the exception of the last which is < 20 mm), with a density of 8.4 g/cm^3 and a fractional mass composition as follows: Cu 75%, Zn 24.533%, Si 0.3%, P 0.01%, Fe 0.1%, Sb, 0.005%, Pb 0.05%, Bi 0.002%. Layer 0 is a 10 mm thick polyvinyltoluene layer modelled with a density 1.032 g/cm^3 and fractional mass composition: H 8.5292% and C 91.4708%. Other scintillator regions (layers 1–17) are 4 mm thick and represented with a polystyrene plastic scintillator of density 1.05 g/cm^3 and fractional mass composition H 7.7423% and C 92.2577%. Since the energy loss per mass per unit area is more than a factor two higher for hydrogen than for most other materials, the spatial resolution used in the calculation was defined so that the dose estimates were not averaged over regions containing materials other than scintillator layers. For towers 28 and 29, the amount of material in front of the HE varies with azimuthal angle due, primarily, to the rectangular shape of the crystals in the electromagnetic calorimeter. This irregularity is not yet simulated, and the dose is calculated for the average instead. The dose was calculated using an R-Phi-Z mesh, independent of the geometry,

overlaying the HE region. The resolution was selected assuming a phi symmetry and aligned in order to obtain dose values within the scintillator regions only. For the HE there was one phi bin in total, a one mm resolution in Z, and a one cm resolution in R. Predictions for the 4-TeV-per-beam ‘2012’ run use a “Run1” CMS FLUKA model, with a central beam pipe and muon endcap region which is modelled to reflect the configuration at that time.

Since the dose received varies over the surface of the tile, the rapidity-averaged value is used. Using a value averaged over the radius of the tile gives similar results. For layer 1, the dose received by a tile ranged from 0.01 to 0.2 Mrad. For layer 7, the dose received ranged from 0.00005 to 0.03 Mrad.

The doses and dose rates are highest for the tiles closest to the beam line. If the exponential constant D does not depend on dose rate, we would expect the tiles to have the same exponential constant, regardless of dose. Monte Carlo studies based on the optical transport code in GEANT4 [21] shows that the exponential constant does not depend strongly on the tile size. Measurements confirm the results of the simulation. Prior to LHC turn on, tiles constructed of SCSN-81 with dimensions of 5 cm \times 8 cm, 12 cm \times 8 cm, and 20 cm \times 20 cm were irradiated at a ^{60}Co source at Argonne National Laboratory at a relatively high dose rate of 100 krad/hr. The resulting dose constants were 1.9, 1.4, and 0.9 Mrad, respectively. The variation with size is much smaller than that seen with the in situ measurements [22]. The extracted dose constants are not corrected for this effect.

The extracted exponential constant in Mrad is shown in figure 4. The different points, at different dose rates, correspond to different tiles in layers 1 and 7. We see a strong dependence on dose rate, with the tiles with the lowest dose rate having the lowest exponential constant and thus suffering more damage for the same dose than the tiles with higher exponential constants.

We fit the extracted D values from the laser results to a power law with an exponent of 0.5. The results of the fit are included in figure 4. The agreement is good.

3 Results from a low dose rate irradiation at a ^{60}Co source

A rectangular tile with WLS fiber, whose construction was similar to those used in the HE (SCSN-81, and with dimensions of 10 cm by 10 cm, with a 50 cm long mirrored fiber) was irradiated in air using the Michigan Memorial Phoenix ^{60}Co source at the University of Michigan, Ann Arbor, MI. The integrated dose was 300 ± 30 krad accumulated over an irradiation time of 1080 hours, for a dose rate of 0.28 krad/hr. The light output when the tile is exposed to a (different) ^{60}Co source was measured before and after irradiation using a Hamamatsu R580-17 PMT coupled to a Keithley picoammeter. An unirradiated identical tile was used to check the stability of the measurement system. The tile was allowed to recover for 6 days between the exposure and the “after” measurement, so as to measure only the permanent damage.

The resulting exponential constant is shown in figure 4. The dose rate for this measurement was larger than that for any tile in the in situ measurement, and the resulting exponential constant is larger than that obtained from the in situ measurements but much smaller than values obtained from high dose rate reactor exposures discussed in the next section. Its value agrees well with the extrapolation of the trend from the in situ measurements to its dose rate.

4 Comparison to previous results

We compare our results to those from ref. [2]. The authors studied both SCSN-81, which is PS-based, and Bicorn-499-35, which is PVT-based. They irradiated disks with a 0.4 cm thickness and a 1'' diameter with a gamma source. The light output was measured using an alpha source, after allowing time for recovery of the temporary damage. The exponential constant D was obtained, for dose rates below 14 krad/hr, where measurements were made for only one dose value, by reading the values of their data from their graphs of light output, and using eq. (1.1) to solve for D . For higher dose rates, where measurements were made for multiple values of the total dose d , the values of the light output versus dose rate are obtained from the functional form in their table 1. Values with the same dose rate but different dose are then fit with an exponential to obtain D .

The values from ref. [2] have exponential dose constants of tens of Mrad at high dose rate, much higher than the values of a few hundredths of a Mrad at the low dose rates probed in the HE. However, even though the geometry and construction of the scintillators studied in the in situ measurement and the measurements in ref. [2] are quite different, and the dose rates quite different, the functional dependence is similar.

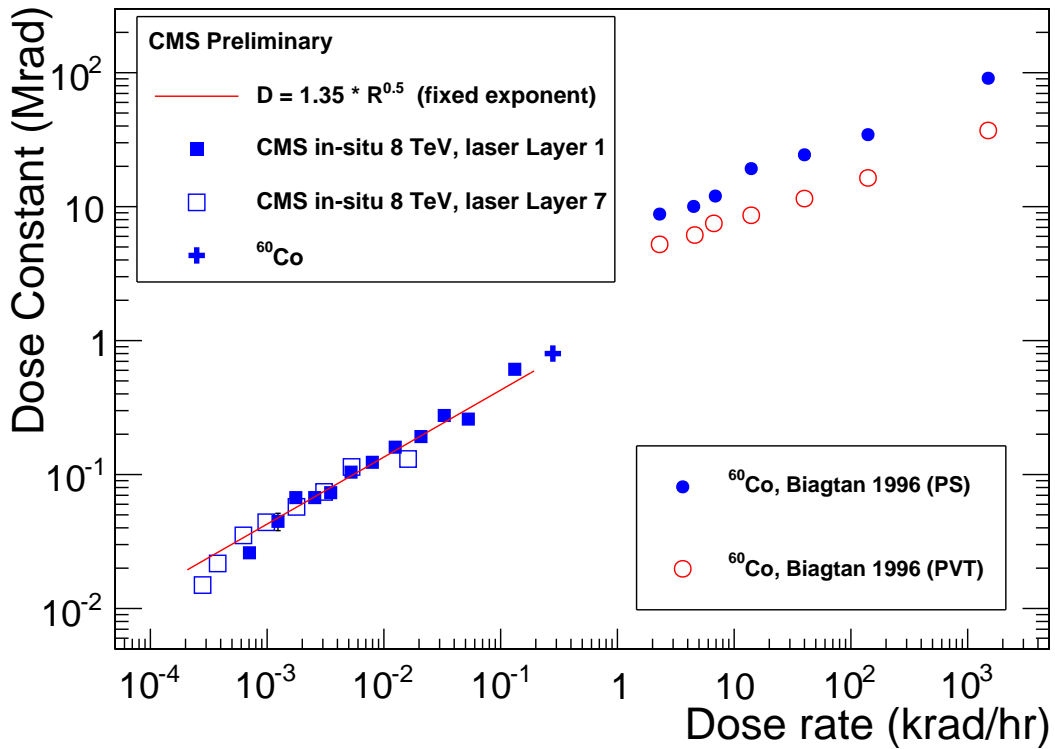


Figure 4. Exponential constant as a function of dose rate. Results from scintillators based on PS are shown in blue, while those based on PVT are shown in red. Results from Layer 1 (7) of the CMS HE scintillator are indicated by filled squares (open squares). Each point corresponds to a different tile pseudorapidity. Results from the ⁶⁰Co irradiations discussed in Biagtan [2] are indicated with circles. The label “⁶⁰Co, CMS” (cross) refers to the measurement first presented in this paper, which was taken using irradiation from a gamma source. A fit to the in situ data to a power law is shown, where the power is set to 0.5.

5 Conclusions

We have looked at the dependence of the light loss for scintillator tiles installed in the CMS endcap hadron calorimeter as a function of both dose and dose rate. We see a power law dependence consistent with that predicted by diffusion of oxygen (or other gas) into the scintillator. We see the functional form is in reasonable agreement with results from gamma source irradiations both by us and by the authors of ref. [2].

Acknowledgments

We would like to thank the CMS BRIL group for doing the FLUKA calculation and the staffs at the Michigan Memorial Phoenix source and the Argonne source for their help. We congratulate our colleagues in the CERN accelerator departments for the excellent performance of the LHC and thank the technical and administrative staffs at CERN and at other CMS institutes for their contributions to the success of the CMS effort. In addition, we gratefully acknowledge the computing centres and personnel of the Worldwide LHC Computing Grid for delivering so effectively the computing infrastructure essential to our analyses. Finally, we acknowledge the enduring support for the construction and operation of the LHC and the CMS detector provided by the following funding agencies: BMWFW and FWF (Austria); FNRS and FWO (Belgium); CNPq, CAPES, FAPERJ, and FAPESP (Brazil); MES (Bulgaria); CERN; CAS, MoST, and NSFC (China); COLCIENCIAS (Colombia); MSES and CSF (Croatia); RPF (Cyprus); SENESCYT (Ecuador); MoER, ERC IUT and ERDF (Estonia); Academy of Finland, MEC, and HIP (Finland); CEA and CNRS/IN2P3 (France); BMBF, DFG, and HGF (Germany); GSRT (Greece); OTKA and NIH (Hungary); DAE and DST (India); IPM (Iran); SFI (Ireland); INFN (Italy); MSIP and NRF (Republic of Korea); LAS (Lithuania); MOE and UM (Malaysia); BUAP, CINVESTAV, CONACYT, LNS, SEP, and UASLP-FAI (Mexico); MBIE (New Zealand); PAEC (Pakistan); MSHE and NSC (Poland); FCT (Portugal); JINR (Dubna); MON, RosAtom, RAS and RFBR (Russia); MESTD (Serbia); SEIDI and CPAN (Spain); Swiss Funding Agencies (Switzerland); MST (Taipei); ThEPCenter, IPST, STAR and NSTDA (Thailand); TUBITAK and TAEK (Turkey); NASU and SFFR (Ukraine); STFC (United Kingdom); DOE and NSF (U.S.A.).

References

- [1] C. Zorn, *Plastic and liquid organic scintillators*, in *Instrumentation in High Energy Physics*, 2nd Edition, F. Sauli ed., [World Scientific](#) (1993), chapter 4, pp. 218–279.
- [2] E. Biagtan, E. Goldberg, R. Stephens, E. Valeroso and J. Harmon, *Gamma dose and dose rate effects on scintillator light output*, *Nucl. Instrum. Meth.* **B 108** (1996) 125.
- [3] U. Holm and K. Wick, *Radiation Stability of Plastic Scintillators and Wave Length Shifters*, *IEEE Trans. Nucl. Sci.* **36** (1989) 579.
- [4] K. Wick, D. Paul, P. Schröder, V. Stieber and B. Bicken, *Recovery and dose rate dependence of radiation damage in scintillators, wavelength shifters and light guides*, *Nucl. Instrum. Meth.* **B 61** (1991) 472.
- [5] B. Bicken, U. Holm, T. Marckmann, K. Wick and M. Rohde, *Recovery and permanent radiation damage of plastic scintillators at different dose rates*, *IEEE Trans. Nucl. Sci.* **38** (1991) 188.

- [6] B. Bicken, A. Dannemann, U. Holm, T. Neumann and K. Wick, *Influence of temperature treatment on radiation stability of plastic scintillator and wavelength shifter*, *IEEE Trans. Nucl. Sci.* **39** (1992) 1212.
- [7] A.D. Bross and A. Pla-Dalmau, *Radiation damage of plastic scintillators*, *IEEE Trans. Nucl. Sci.* **39** (1992) 1199.
- [8] N. Giokaris, M. Contreras, A. Pla-Dalmau, J. Zimmerman and K.F. Johnson, *Study of dose-rate effects on the radiation damage of polymer-based SCSN23, SCSN81, SCSN81+Y7, SCSN81+Y8 and 3HF scintillators*, *Radiat. Phys. Chem.* **41** (1993) 315.
- [9] CMS collaboration, *The CMS hadron calorimeter project: Technical Design Report*, [CERN-LHCC-97-031](#) (1997) [CMS-TDR-2].
- [10] T. Förster, *Zwischenmolekulare energiewanderung und fluoreszenz*, *Ann. Phys.* **437** (1947) 55.
- [11] T. Seguchi, S. Hashimoto, K. Arakawa, N. Hayakawa, W. Kawakami and I. Kuriyama, *Radiation induced oxidative degradation of polymers — I: Oxidation region in polymer films irradiated in oxygen under pressure*, *Radiat. Phys. Chem.* **17** (1981) 195.
- [12] W. Busjan, K. Wick and T. Zoufal, *Shortlived absorption centers in plastic scintillators and their influence on the fluorescence light yield*, *Nucl. Instrum. Meth.* **B 152** (1999) 89.
- [13] P.C. Trimmer, J.B. Schlenoff and K.F. Johnson, *Spatially resolved uv-vis characterization of radiation-induced color centers in poly(styrene) and poly(vinyltoluene)*, *Radiat. Phys. Chem.* **41** (1993) 57.
- [14] N. Emanuel and A. Buchachenko, *Chemical Physics of Polymer Degradation and Stabilization*, VNU Science Press (1987).
- [15] CMS collaboration, *The CMS experiment at the CERN LHC*, [2008 JINST 3 S08004](#).
- [16] P. Cushman, A. Heering and A. Ronzhin, *Custom HPD readout for the CMS HCAL*, *Nucl. Instrum. Meth.* **A 442** (2000) 289.
- [17] T. Shaw et al., *Front end readout electronics for the cms hadron calorimeter*, *IEEE Nucl. Sci. Symp. Conf. Rec.* **1** (2002) 194.
- [18] CMS collaboration, *Absolute Calibration of the Luminosity Measurement at CMS: Winter 2012 Update*, [CMS-PAS-SMP-12-008](#) (2012).
- [19] A. Ferrari, P.R. Sala, A. Fasso and J. Ranft, *FLUKA: A multi-particle transport code (program version 2005)*, [CERN-2005-010](#) (2005) [INFN-TC-2005-11] [SLAC-R-773].
- [20] T.T. Bohlen et al., *The fluka code: Developments and challenges for high energy and medical applications*, *Nucl. Data Sheets* **120** (2014) 211.
- [21] GEANT4 collaboration, S. Agostinelli et al., *GEANT4: A Simulation toolkit*, *Nucl. Instrum. Meth.* **A 506** (2003) 250.
- [22] P. De Barbaro, CMS IN-2008/022, private communication.